JOURNAL OF BACTERIOLOGY, Apr. 2000, p. 2001–2009 Vol. 182, No. 7
0021-9193/00/$04.00+0

Pyruvate Kinase of the Hyperthermophilic Crenarchaeote *Thermoproteus tenax*: Physiological Role and Phylogenetic Aspects

ALEXANDER SCHRAMM,[1] BETTINA SIEBERS,[1] BRITTA TJADEN,[1] HENNER BRINKMANN,[2] AND REINHARD HENSEL[1]*

Department of Microbiology, Universität GH Essen, D-45117 Essen,[1] and Institute of Evolutionary Biology, Department of Biology, Universität Konstanz, D-78547 Konstanz,[2] Germany

Received 21 September 1999/Accepted 7 January 2000

Pyruvate kinase (PK; EC 2.7.1.40) of *Thermoproteus tenax* was purified to homogeneity, and its coding gene was cloned and expressed in *Escherichia coli*. It represents a homomeric tetramer with a molecular mass of 49 kDa per subunit. PK exhibits positive binding cooperativity with respect to phosphoenolpyruvate and metal ions such as Mg^{2+} and Mn^{2+}. Heterotropic effects, as commonly found for PKs from bacterial and eucaryal sources, could not be detected. The enzyme does not depend on K^+ ions. Heterotrophically grown cells exhibit specific activity of PK four times higher than autotrophically grown cells. Since the mRNA level of the PK coding gene is also accordingly higher in heterotrophic cells, we conclude that the PK activity is adjusted to growth conditions mainly on the transcript level. The enzymic properties of the PK and the regulation of its expression are discussed with respect to the physiological framework given by the *T. tenax*-specific variant of the Embden-Meyerhof-Parnas pathway. *T. tenax* PK shows moderate overall sequence similarity (25 to 40% identity) to its bacterial and eucaryal pendants. Phylogenetic analyses of the known PK sequences result in a dichotomic tree topology that divides the enzymes into two major PK clusters, probably diverged by an early gene duplication event. The phylogenetic divergence is paralleled by a striking phenotypic differentiation of PKs: PKs of cluster I, which occur in eucaryal cytoplasm, some gamma proteobacteria, and low-GC gram-positive bacteria, are only active in the presence of fructose-1,6-bisphosphate or other phosphorylated sugars, whereas PKs of cluster II, found in various bacterial phyla, plastids, and in *Archaea*, show activity without effectors but are commonly regulated by the energy charge of the cell.

As shown by several investigations, *Archaea* use the Embden-Meyerhof-Parnas (EMP) pathway for carbon metabolism, and in some archaeal species (the genera *Pyrococcus*, *Thermococcus*, *Desulfurococcus*, and *Thermoproteus*) the catabolic EMP pathway represents the main route for glucose degradation (37, 40). So far, in thermophilic *Archaea* only variants of the classical EMP pathway have been found. Common to these variants is the irreversible oxidation step transforming glyceraldehyde-3-phosphate directly to 3-phosphoglycerate by a ferredoxin-dependent glyceraldehyde-3-phosphate oxidoreductase (GAP:FdOR) found in *Pyrococcus*, *Thermococcus*, and *Desulfurococcus* strains (37, 43) or by a nonphosphorylating NAD^+-dependent glyceraldehyde-3-phosphate dehydrogenase (GAPN) found in *Thermoproteus tenax* (4, 15, 38). These enzymes substitute for the combined action of conventional phosphorylating—but reversible—glyceraldehyde-3-phosphate dehydrogenase (GAPDH) and 3-phosphoglycerate kinase, which, however, allows ATP formation.

We chose *T. tenax*, a hyperthermophilic, facultatively heterotrophic member of the kingdom *Crenarchaeota*, as an object for regulatory studies on archaeal carbohydrate metabolism. *T. tenax* is able to grow chemolithoautotrophically on CO_2, H_2 and S^0, as well as chemoorganoheterotrophically in the presence of S^0 and carbohydrates such as glucose, starch, and amylose (45). The variant of the EMP pathway in *T. tenax* is characterized by a bidirectionally working, nonallosteric pyrophosphate-dependent 6-phosphofructokinase (PP_i-PFK) and by two GAPDHs differing in their cosubstrate specificity (15, 39). Whereas the phosphorylating $NADP^+$-dependent GAPDH seems to fulfill a role in gluconeogenesis (N. A. Brunner, B. Siebers, and R. Hensel, manuscript in preparation), functional analyses of the NAD^+-dependent GAPDH (GAPN) of *T. tenax* revealed that this enzyme is involved in glycolysis and represents a central control point of the pathway (4). With its regulatory properties (allosteric inhibition by NADP(H), NAD(H), and ATP; allosteric activation by AMP, ADP, glucose-1-phosphate, and fructose-6-phosphate), the enzyme seems to compensate for the missing regulatory potential of PFK. To investigate whether the integration of an irreversible, highly regulated GAPN in the catabolic EMP pathway of *T. tenax* impacts the functional phenotype of PK, usually the second site of glycolytic regulation, we focused on the enzymic properties of PK and its expression in response to growth conditions.

In *Bacteria* and *Eucarya*, the enzyme is functionally and structurally well characterized. In all *Eucarya* spp. investigated so far and some bacteria, the activity of PK depends on the presence of fructose-1,6-bisphosphate or other sugar phosphates, whereas PKs of the majority of bacteria and plastids show basal activity without effectors and are mostly regulated by adenosine phosphates (i.e., by the energy charge of the cell). More than 50 primary structures of bacterial and eucaryal enzymes are available in databases. Three-dimensional structures have been determined for one bacterial and three eucaryal enzymes (18, 24, 26, 29). Recently, the mode of ATP binding (23) and allosteric activation of PK by FBP were described at the atomic level (18). The enzyme is a homotetramer

* Corresponding author. Mailing address: FB 9 Mikrobiologie, Universität GH Essen, Universitätsstr. 5, 45117 Essen, Germany. Phone: 49-201-183-3442. Fax: 49-201-183-3990. E-mail: r.hensel@uni-essen.de.

in almost all organisms, although dimeric PKs have been reported for *Schizosaccharomyces pombe* (30, 31) and *Zymomonas mobilis* (32). Each subunit folds into four distinct domains (designated N, A, B, and C). The first domain, N, is characterized by a short α-helix at the N terminus, which, however, is absent in some bacterial PKs, such as the FBP-activated enzyme of *Escherichia coli* (26). The catalytical A domain folds into the common symmetrical α/β_8-barrel, sharing this topology with two other glycolytic enzymes: triosephosphate isomerase and aldolase. The third domain, B, consists of a small β-barrel forming a cap over the active site. Finally, domain C located at the C terminus exhibits an α/β open-sheet motif and usually displays regulatory functions. In contrast to bacterial and eucaryal enzymes, little is known about the structure and function of archaeal PKs. Up to now only the enzymic properties of the PK of *Thermoplasma acidophilum* could be determined (34). The enzyme represents a homomeric tetramer with a molecular mass of 250 kDa and displays cooperative substrate binding; its substrate affinity is increased by AMP. Genome sequencing projects published so far have revealed the presence of PK coding genes (*pyk*) in *Pyrobaculum aerophilum* (11), *Methanococcus jannaschii* (5), and *Pyrococcus horikoshii* (19), but no information on the enzymic properties of these enzymes is available. By analyzing *T. tenax* PK, we wanted to better understand the control mechanisms governing the central carbon metabolism of that organism and to get better insights into the structure and function of the archaeal PK in general.

MATERIALS AND METHODS

Chemicals and plasmids. Phosphoenolpyruvate (PEP) and rabbit muscle lactate dehydrogenase (LDH) were from Sigma, Munich, Germany. ADP, ATP, NAD^+-NADH, and $NADP^+$-NADPH were purchased from Gerbu, Gaiberg, Germany. All other chemicals (Pro Analysis grade) were from Sigma, Fluka, or Merck. Cloning of genomic DNA was performed with plasmids pUC19 (MBI Fermentas) and pBluescript IIKS(+) (Stratagene). For heterologous expression, the vector pJF118EH (13) was used.

Bacterial strains and growth conditions. Mass cultures of *T. tenax* Kra 1 (DSM 2078) were grown as described previously (38). For cloning and expression experiments, *E. coli* DH5α (Life Technologies) was grown as described earlier (36).

Enzyme assay. The standard assay was performed at 50 or 60°C with 100 mM Tris-HCl (pH 7.0) at the respective temperature, 0.5 mM NADH, 4 U of LDH (rabbit muscle; Sigma), 20 mM PEP, 5 mM ADP, and 10 mM $MgCl_2$. Enzyme activity was measured by monitoring the decrease in absorption at 366 nm. Reactions were started by adding the heat-labile substrate PEP (Fig. 1). Enzyme concentrations ranged from 2 to 10 μg of protein/ml. The enzyme reaction was monitored for the first 1 to 2 min.

Purification of PK from *T. tenax*. Preparation of crude extracts from *T. tenax*, heat treatment, ion-exchange chromatography, and hydrophobic interaction chromatography were performed as described previously (40). Fractions containing PK activity were pooled, dialyzed against 50 mM HEPES-KOH (pH 7.0) containing 10 mM 2-mercaptoethanol and 300 mM KCl, concentrated by membrane filtration (Centricon 30; Amicon), and subjected to gel filtration on a HiLoad 26/60 Superdex column (Pharmacia; 60 by 2.6 cm; flow rate, 0.7 ml/min) equilibrated in the same buffer. Pooled fractions containing PK activity were dialyzed and applied to a AMP-Sepharose column (Sigma; 6 by 1 cm; flow rate, 0.2 ml/min) equilibrated with 50 mM HEPES (pH 7.0) and 10 mM 2-mercaptoethanol. Homogeneous protein was eluted by equilibration buffer containing 100 mM KCl. Sodium dodecyl sulfate-polyacrylamide gel electrophoresis (SDS-PAGE) as described earlier (22). Determination of protein concentration was done by using the DC Protein Assay (Bio-Rad).

Molecular mass determination. The native molecular mass was determined by gel filtration on a HiLoad 26/60 Superdex 200 preparatory-grade column (Pharmacia) as described elsewhere (40). The molecular mass of subunits was determined by denaturating SDS-PAGE with SDS-7 Marker (Sigma) as the standard.

CNBr fragmentation and protein sequencing. Because the enzyme turned out to be N-terminally blocked, the protein was cleaved with CNBr (27). Resulting peptides were separated by isoelectric focusing in the first dimension and by tricine-SDS-PAGE in the second dimension as described previously (14). Peptides and proteins were immobilized on ProBlott membranes (Applied Biosystems) by semidry electrotransfer (10). Sequencing was performed by automated Edman degradation with a gas-phase Sequenator 473A (Applied Biosystems). The partial sequence of the following two peptides were determined: peptide 1, RPLQITAGARVSFKLAEKGDGFVPVPRREFF; and peptide 2, LDGKLVL RIISAAQ.

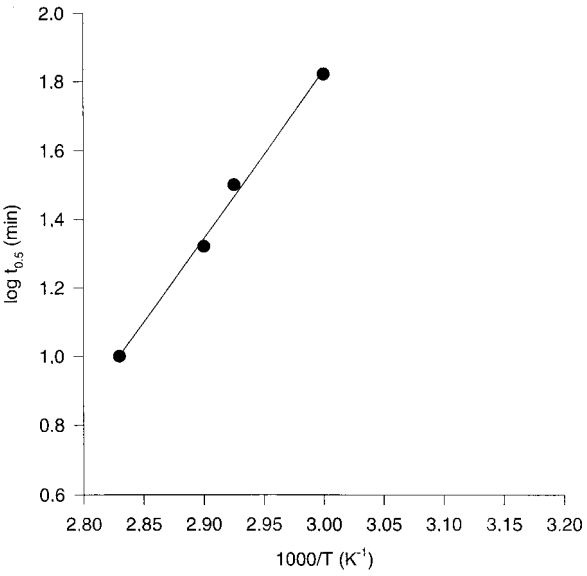

FIG. 1. Arrhenius plot of PEP decay. A solution containing 50 mM HEPES (pH 7.0)–10 mM PEP was incubated at various temperatures, and the residual PEP concentration was determined by the enzyme assay described in the text.

Cloning and sequencing of the coding gene. Genomic DNA was prepared as described earlier (44), as modified by Meakin et al. (28). The gene encoding PK was identified by hybridization with a degenerated oligonucleotide 5′-TTAGAT GGIAARYTNGT3′ deduced from the hexapeptide LDGKLV. For hybridization, the oligonucleotide was labeled with digoxigenin according to the manufacturer's instructions (Roche Diagnostics). DNA was transferred to nylon membranes (Nytran; Schleicher & Schuell) by capillary blotting (6). Southern blots were hybridized at room temperature in 5× SSC (1× SSC is 0.15 M NaCl plus 0.015 M sodium citrate) and washed two times at 37°C in 1× SSC. A strongly hybridizing 3-kb *Bam*HI/*Hin*dIII-fragment was selected, cloned, and sequenced with the aid of an Automated Laser Fluorescence DNA Sequencer (Amersham Pharmacia).

Expression of the *pyk* gene from *T. tenax* in *E. coli*. For expression of the *pyk* gene, the coding region was cloned into pJF118EH via two new restriction sites (*Eco*RI and *Bam*HI) created with the mutagenic primers 5′-GATCGCGCGAG TAGAATTCATGTTCAC-3′ and 5′-GTTTACTCAGGGATCCGTAATTTAA TAG-3′. The sequence of the clone expressing the *pyk* gene was confirmed by sequencing of both strands. Expression in *E. coli* DH5α cells was performed by standard procedures (36).

Purification of *T. tenax* PK from transformed *E. coli*. First, 5 g of *E. coli* cells was resuspended in 10 mM potassium phosphate buffer (pH 7.3) containing 30 mM 2-mercaptoethanol and passed three times through a French press cell at 150 MPa. Then, after centrifugation (20,000 × *g* for 30 min), the supernatant was heat precipitated (80°C for 30 min) and centrifuged again. Homogeneous enzyme preparations were obtained by chromatography on AMP-Sepharose as outlined above for the enzyme prepared from *T. tenax*.

Northern blot analyses. Total RNA was prepared from autotrophically and heterotrophically grown cells by using TRIzol reagent according to the manufacturer's instructions (Life Technologies, Eggenstein, Germany). The integrity of the RNA was routinely checked by agarose gel electrophoresis by using a morpholine propane sulfonic acid (MOPS)–6% formaldehyde buffer system, and the concentration was determined spectrophotometrically at λ = 260 nm. Digoxigenin-labeled antisense mRNA was obtained by in vitro transcription from the T7 promoter of vector pSPT 19 (Roche Diagnostics). For that purpose, the coding region of the *T. tenax pyk* gene was inserted into the *Eco*RI/*Bam*HI restriction sites of the vector. Hybridization was carried out at 68°C overnight in DIG Easy Hyb solution (Roche Diagnostics), and stringency washes were performed in 0.1× SSC–0.1% SDS at 68°C. Densitometric analyses were performed by using a laser densitometer Ultroscan XL (Pharmacia LKB) according to the manufacturer's instructions.

Primer extension analyses. Primer extension was performed by using a protocol of Kuo et al. (21), with the modification that the hybridization buffer contained 0.3 M KCl, 2 mM EDTA, and 20 mM Tris-HCl buffer (pH 8.3). RNA from heterotrophically as well as from autotrophically grown cells of *T. tenax* was used as a source for cDNA synthesis. To map the *pyk* transcription start site, the 5′-^{32}P-labeled antisense oligonucleotide PK1PEX (5′-CCTCCGATGGCGATG

TABLE 1. Purification of PK from *T. tenax*

Fraction	Total protein (mg)	Total activity (U)	Sp act (U/mg of protein)	Purification (fold)	Yield (%)
Crude extract	876	79	0.09		100
Heat precipitation	690	83	0.12	1.3	105
Q-Sepharose	117	78	0.7	7.2	99
Phenyl-Sepharose	21	49	2.3	25.5	63
Gel filtration	6	31	5.4	59	40
AMP-Sepharose	0.2	9	45	490	12

CGT-3′), which is complementary to positions 103 to 120 of the *pyk* gene, was used as primer for cDNA synthesis and accompanying sequencing reactions. The labeled cDNA products were analyzed on a denaturating polyacrylamide gel (5%), along with a sequence ladder generated with the same oligonucleotide as the primer.

Sequence handling and phylogenetic analyses. Homology searches were performed with BLASTN at The National Center for Biotechnology Information (NCBI; http://www.ncbi.nlm.nih.gov/BLAST). Sequences were extracted from GenBank or from the NCBI, i.e., the Microbial Genome Database (http://www.ncbi.nlm.nih.gov/BLAST/unfinishedgenome.html), and first aligned with CLUSTAL W (42). This alignment was refined manually by using the MUST program package (33). Regions of uncertain alignment were omitted, leaving 462 amino acid positions for analysis. For the phylogenetic tree the topology of the Maximum Parsimony Bootstrap analysis was used, obtained by PAUP version 4.0d65 with 500 bootstrap replicates and four-times-random addition (41). Maximum likelihood analyses were performed by using MOLPHY version 2.3 (1), starting with the NJDIST tree, using the local rearrangement option (data not shown). Distance analysis were performed with the MUST package using the Kimura correction and the neighbor-joining method (35), including 1,000 bootstrap replicates. The *T. tenax pyk* gene sequence is deposited at GenBank (AF065890).

RESULTS

Specific activity of PK in autotrophically and heterotrophically grown *T. tenax* cells, purification of the enzyme, and molecular mass determination. As revealed from measurements with dialyzed crude extracts, cells grown in the presence of glucose showed a specific activity of PK approximately four times higher (0.17 U/mg) than cells grown with CO_2 as the only carbon source (0.04 U/mg of protein), thus supporting its catabolic function. From 15 g (wet weight) of heterotrophically grown cells, 0.2 mg of homogeneous protein was recovered with a specific activity of 45 U/mg, a value corresponding to a recovery of 12% (Table 1). The enzyme migrated as a single band on SDS-PAGE with an apparent molecular mass of 48 kDa (Fig. 2). Molecular mass determination under nondenaturating conditions yielded values of 200 + 10 kDa, indicating that the PK of *T. tenax* is a homomeric tetramer like the majority of PKs known.

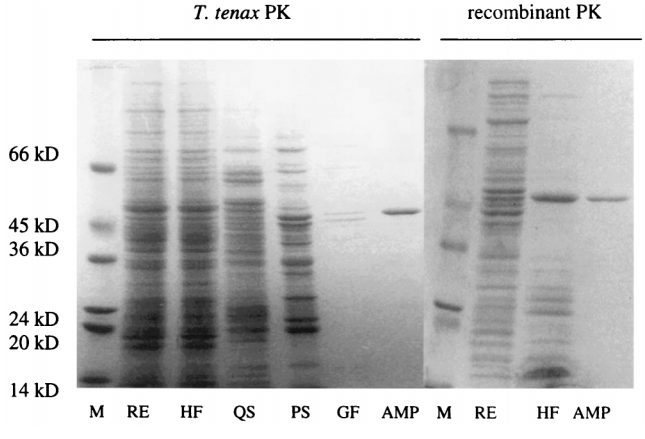

FIG. 2. Purification of PK from *T. tenax* and of recombinant PK. (M, marker; RE, crude extract; HF, heat precipitation; QS, anion-exchange chromatography; PS, hydrophobic interaction chromatography; GF, gel filtration; AMP, AMP-Sepharose).

Nucleotide sequence of the *pyk* gene and its flanking regions. Southern hybridizations with a degenerated oligonucleotide probe derived from the N-terminal sequence of a CNBr-fragment of the protein gave a strong positive signal with a 3-kb *Bam*HI/*Hin*dIII fragment of the genomic DNA of *T. tenax*. Subsequent sequencing revealed two open reading frames (see GenBank accession no. AF065890). One of them was identified as a *pyk* gene by correspondence of the deduced amino acid sequence with the partial peptide sequence and by sequence similarity with known PKs from *Bacteria* and *Eucarya*. The second open reading frame starting 116 bp downstream of the *pyk* gene (i.e., the same direction as *pyk*) showed 35 to 50% identity to cysteinyl-tRNA synthetases from other organisms of the three domains of life.

The *pyk* gene of *T. tenax* consists of 1,341 bases coding for a 49-kDa polypeptide of 446 residues (start codon, GTG; stop codon, TAA). The G+C content has been calculated to be 56%, a value corresponding very well with the average G+C content of the *T. tenax* genome (55.9% [25]). Southern hybridizations using a 1.3-kb *Sac*I fragment comprising the major part of the *pyk* gene as a probe resulted only in a single positive signal with the genomic DNA digested with several restriction enzymes (data not shown), indicating the presence of a single *pyk* homologue in *T. tenax*.

Deduced amino acid sequence of PK. Comprising only 446 residues, the *T. tenax* enzyme represents one of the shortest PK sequences known. Like the protein sequences deduced from the putative *pyk* genes of the *Archaea P. horikoshii* and *M. jannaschii*, the PK sequence of *T. tenax* is about 10% shorter than those of *Bacteria* and *Eucarya*. In an alignment with 52 representatives of the three domains of life, the sequence of the *T. tenax* PK showed overall amino acid identities ranging from 27 to 42%. The comparison revealed that the catalytically essential residues (ARGDL) at positions 236 to 240 and residues involved in subunit binding (PTRAE) at positions 283 to 287 (Fig. 3; assigned on the basis of three-dimensional analyses of the PK from yeast [18]) are conserved in the *T. tenax* enzyme. These conservative residues are located in the domains A and B. Surprisingly, no preferred similarity to the translated sequences of the putative *pyk* genes of the *Archaea P. aerophilum*, *M. jannaschii*, and *P. horikoshii* were observed: the archaeal sequences neither shared specific sequence signatures nor showed significantly higher identity values with each other (28.4 to 36.2% identity) than with the homologues of *Bacteria* or *Eucarya*.

Transcript analyses. Northern blot analyses with total RNA from autotrophically and heterotrophically grown cells using antisense *pyk* mRNA as a probe resulted in a strong hybridization signal with a 1.3-kb and—to a significantly lesser extent—with a 1.6-kb transcript (Fig. 4A). As revealed by densitometric analyses, the 1.3-kb transcript gave a signal approximately four times stronger with heterotrophic cells compared to autotrophic cells, thus corresponding well with the fourfold-higher PK activity in heterotrophically grown cells. In contrast, the signal of the 1.6-kb transcript remained at a rather low level under both growth conditions (Fig. 4A). Whether this significantly weaker signal can be assigned to a transcript initiated from an alternative promoter of the *pyk* gene is currently being analyzed.

Using the oligonucleotide binding at positions 103 to 120 of the *pyk* gene, the start site of the shorter transcript was deter-

```
                      A                                          B
            83    Bb1 92   | 257  Aβ6        Aα6             Aβ7    Aα7       Aα7´                   341
YEAST       LDTKGPEIRT     |  TDGVMVARGDLGIEIPAPEVLAVQKKLIAKSNLAGKPVICATQMLESMTYNPRPTRAEVSDVGNAILDGADCVMLSGETAKGNYP
CAEEL       LDTKGPEIRT     |  SDGVMVARGDLGIEIPAEKVFLAQKMLISKCNRAGKPVICATQMLESMVHKPRPTRAEGSDVANAVLDGADCVMLSGETAKGEYP
ECOLI1      LDTKGPEIRT     |  SDGIMVARGDLGVEIPVEEVIFAQKMMIEKCIRARKVVITATQMLDSMIKNPRPTRAEAGDVANAILDGTDAVMLSGESAKGKYP
ECOLI2      GDLQGPKIRV     |  SDVVMVARGDLGVEIGDPELVGIQKALIRRARQLNRAVITATQMMESMITNPMPTRAEVMDVANAVLDGTDAVMLSAETAAGQYP
METJA       MDLKGIKIRI     |  SDGVMVARGDLGVEVPIENIPIEQKNILRIANRYGILSITATQILDSMINNPFPTRAEVTDIANAIYDGTDCLMLSNETTIGKYP
THETX       ADLRGPSVRT     |  ADYIVIARGDLALHYGLEYIPKVQRLLVERSLSAGRPVAVATQLLDSMQTNTTPTRAEVNDVYTTASLGVDSLWLTNETASGEHP
              *  *   *     |   *    *****              *                 ***  **      *****  *         * *  *  *   *  *
```

FIG. 3. Partial sequence alignment of PK from *T. tenax* with PKs from eucaryal, bacterial, and archaeal representatives. GenBank entries: YEAST, *S. cerevisiae* (U12980); CAEEL, *C. elegans* (Z69385); ECOLI1, *E. coli* PK1 (AE000262); ECOLI2, *E. coli*; PK2 (AE000279); METJA, *M. jannaschii* (U67468). THETX, *T. tenax* (the present study). Conserved residues are marked with an asterisk. Residues in boldface type indicate potassium binding sites (A) or subunit and metal binding sites (B), respectively. The secondary structure elements above the sequences are deduced from the three-dimensional structure of yeast enzyme (18).

mined to be at the thymidine immediately in front of the gene (Fig. 4B). Corresponding with the Northern blot signals observed with the 1.3-kb transcript, the primer extension signal with RNA from cells grown under heterotrophic conditions showed a significantly higher intensity than that obtained with autotrophically grown cells, thus confirming the higher *pyk* transcript level in heterotrophic cells.

Heterologous expression of the *pyk* gene. For functional and structural investigations, the *pyk* gene was expressed in *E. coli*. About 1 mg of homogeneous enzyme could be obtained from 1 g (wet weight) of recombinant *E. coli* DH5α cells. As shown in Fig. 2 and Table 2, the enzyme isolated from *T. tenax* and from transformed *E. coli* exhibited virtually the same properties with respect to molecular mass and the kinetic parameters for substrate, cosubstrate, and Mg^{2+} saturation, indicating a highly similar phenotype for both enzymes. Therefore, the screening experiments for ligands influencing the enzymic properties were performed with the better available recombinant enzyme.

Enzymic properties. The enzyme assays were conducted at only 50°C because of the heat-labile mesophilic auxiliary enzyme used in the coupled optical test. Like known PKs, the enzyme of *T. tenax* showed an absolute requirement for divalent cations. However, of the metal ions tested (Mg^{2+}, Mn^{2+}, Co^{2+}, Fe^{2+}, Ni^{2+}, and Cd^{2+}), activity could only be observed with Mg^{2+}, Mn^{2+}, and Co^{2+}. The highest V_{max} values were obtained with Mn^{2+} and Mg^{2+} (Table 2). Co^{2+} allowed only one-tenth of the maximal activity.

Saturation kinetics were followed with Mg^{2+}, Mn^{2+}, PEP, and ADP. Whereas the enzyme exhibited classical saturation kinetics with cosubstrate, sigmoidal saturation curves were obtained with substrate and metal ions, indicating the positive cooperative binding of these ligands (Fig. 5 and Table 2). Mg^{2+} showed the highest binding cooperativity measured at all (Hill

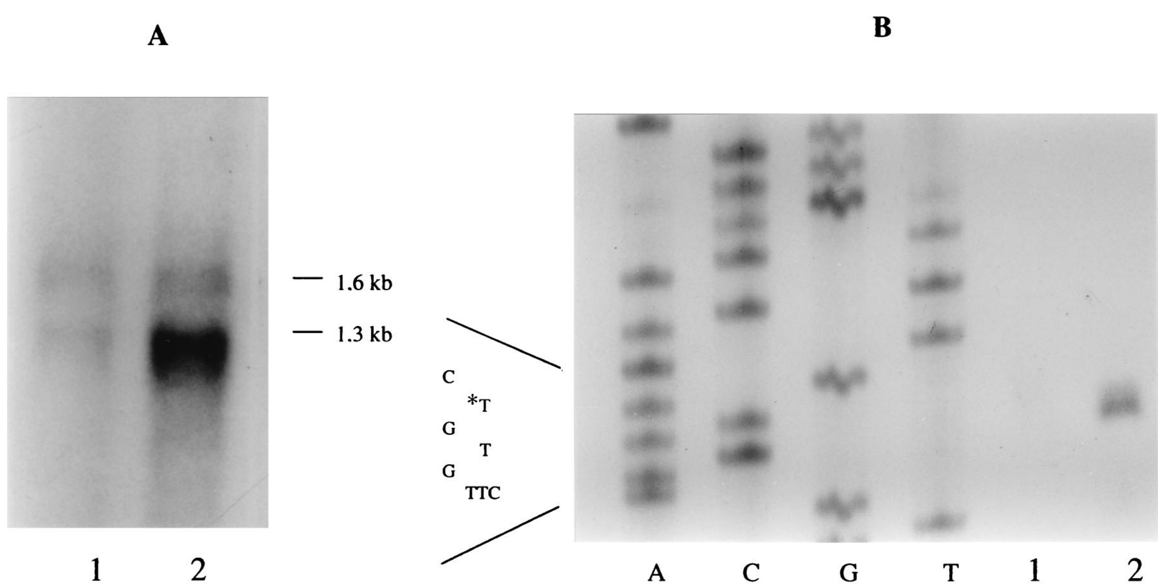

C
```
      -25                                 +1
CTTCATATAAATAAAGATCGCGCGAGTAGTATCTGTGTTCACTAAAATTGTAGCTACATT
```

FIG. 4. Northern blot analysis of *pyk* mRNA and determination of the transcript start site. (A) Northern blot analysis of *pyk* transcripts with RNA from autotrophically (lane 1) and heterotrophically (lane 2) grown cells probed with *pyk* antisense mRNA. (B) Mapping of the *pyk* transcription start by primer extension. The transcript begins at position −1 with regard to the start codon of the *pyk* gene (marked by an asterisk). The primer extension products from autotrophically grown cells (lane 1) and heterotrophically grown cells (lane 2), together with the sequence ladder (lanes A, C, G, and T), are shown. (C) Nucleotide sequence of the sense strand of the *pyk* region. The position of a putative box A promoter element (marked in boldface) and the starting point of transcription (marked by an arrow) are indicated.

TABLE 2. Biochemical properties of the PK of *T. tenax* and transformed *E. coli*[a]

Property	PK isolated from:	
	T. tenax	Transformed *E. coli*
Mol wt		
M_r, native (gel filtration)	195,000	200,000
M_r, subunits (SDS-PAGE)	48,000	48,000
Calculated	49,075	
ADP saturation		
K_m (mM)	0.7*	0.7*
V_{max} (U/mg)	45	45
Hill coefficient (h)	ND	1.0
PEP saturation		
$S_{0.5}$ (mM)	3**	3**; 0.8†
V_{max} (U/mg)	45**	46**,†
Hill coefficient (h)	ND	2.0**; 1.6†
Mg^{2+} saturation		
$S_{0.5}$ (mM)	4.8‡	5.5‡
V_{max} (U/mg)	42‡	46‡
Hill coefficient (h)	ND	2.8
Mn^{2+} saturation		
$S_{0.5}$ (mM)	ND	0.8‡
V_{max} (U/mg)	ND	45‡
Hill coefficient (h)	ND	1.6

[a] Assay conditions were as follows: 100 mM Tris-HCl (pH 7) at 50°C, 0.5 mM NADH, and 4 U of LDH. Concentrations of the invariable substrates are indicated as follows: *, 20 mM PEP, 10 mM $MgCl_2$; **, 5 mM ADP, 10 mM $MgCl_2$; †, 5 mM ADP, 5 mM $MnCl_2$; and ‡, 20 mM PEP, 5 mM ADP. ND, not determined. $S_{0.5}$, concentration at half-maximal saturation.

coefficient [h] = 2.8). The cooperativity of substrate binding was dependent on the metal ion added and was more pronounced in the presence of Mg^{2+} (h = 2.0) than with Mn^{2+} (h = 1.6). The activity of the enzyme did not depend on potassium ions.

None of the common effectors of known PKs influenced the activity of *T. tenax* PK. Neither activation nor inhibition of the enzyme activity could be observed with the following compounds (concentration range, 10 μM to 10 mM; assay in the presence of half-saturating substrate and cosubstrate concentration): FBP, fructose-6-phosphate, ribose-5-phosphate, glucose-1-phosphate, glucose-6-phosphate, glucose, trehalose, citrate, sedoheptulose-7-phosphate, erythrose-4-phosphate, 3-phosphoglycerate, 2,3-bisphosphoglycerate, glyceraldehyde-3-phosphate, dihydroxyacetone phosphate, $NADP^+$, NADPH, NAD^+, NADH, phenylalanine, alanine, AMP, ATP, P_i, and PP_i.

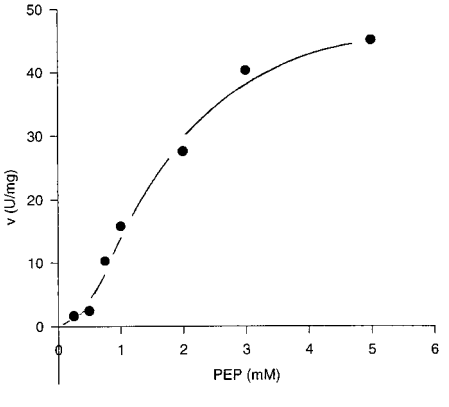

FIG. 5. PEP saturation of the PK of *T. tenax* in the presence of 20 mM $MgCl_2$.

Phylogenetic analyses. Phylogenetic trees were constructed based on the deduced amino acid sequences of 52 *pyk* genes from *Bacteria*, *Eucarya*, and *Archaea* by using maximum parsimony, distance matrix, and maximum likelihood (ML) methods. The tree in Fig. 6 was constructed based on the topology of the PAUP bootstrap consensus tree using the user-defined tree option of the MOLPHY package. All three methods resulted in the same dichotomic tree structure, dividing the PK enzymes into two discrete clusters. PK cluster I contains all sequences of the eucaryal cytoplasm, all sequences of low-GC gram-positive bacteria, and some of the gamma proteobacteria, whereas PK cluster II includes members of most bacterial phyla (except of low-GC gram-positive bacteria), plastids, and *Archaea*.

Generally, the topology of the PK cluster I is supported by fairly good bootstrap values for both maximum parsimony and neighbor-joining analysis. The position of the PK cluster I of *E. coli* and *Salmonella typhimurium*, however, remained ambiguous in being either the closest relatives to the eucaryal PK sequences or in some analysis branching together with the low-GC gram-positive bacteria (ML analysis [data not shown]). In contrast, the deeper branching lineages of PK cluster II are only poorly resolved and are not confirmed by high bootstrap values. The monophyly of *Archaea* could not be confirmed either by neighbor-joining or by ML analysis (data not shown). On the other hand, both the maximum parsimony and the distance matrix methods found several clearly separated groups that are in agreement with rRNA-based phylogeny, e.g., alpha proteobacteria, beta and gamma proteobacteria, high-GC gram-positive bacteria, and low-GC gram-positive bacteria.

DISCUSSION

Functional and structural properties of PK of *T. tenax* and its coding gene. With the *T. tenax* enzyme, an archaeal PK could be assigned for the first time to its coding gene. Common to known PKs, the *T. tenax* enzyme is N-terminally blocked. As shown, however, by comparing the enzymic properties of the PK purified from *T. tenax* with those of the recombinant enzyme, the putative N-terminal modification does not influence the functional properties of PK.

A rather rare feature of PK is that the *T. tenax* enzyme does not depend on potassium ions. Interestingly, one of the two sequence motifs characteristic for K^+ binding in K^+-dependent PKs (LDTKGPEIRT; positions 83 to 92 (Fig. 3); numbering is according to the yeast enzyme [18]) is changed in a similar way, as observed with the K^+-insensitive PKs of *E. coli* (PKII of *E. coli*) and *Corynebacterium glutamicum* (17). The nonsusceptibility of the *T. tenax* PK toward heterotropic effectors also seems rather exceptional. A similar reduced regulatory potential has only been described for the PKs of *Schizosaccharomyces pombe* (30) and *Zymomonas mobilis* (32).

As a consequence of the N-terminal blockage, the translation start of the *T. tenax* PK could not be determined directly. The most probable initiation codon is GUG at positions 261 to 263 (GenBank accession no. AF065890), immediately following the transcription start of the *pyk* gene at T_{260} (Fig. 4C). As shown in several cases, GUG functions also in *Archaea* as (although rare) an initiation triplet coding for methionine. The proposed position of the translation start is confirmed by the observation that the following nucleotide sequence codes for

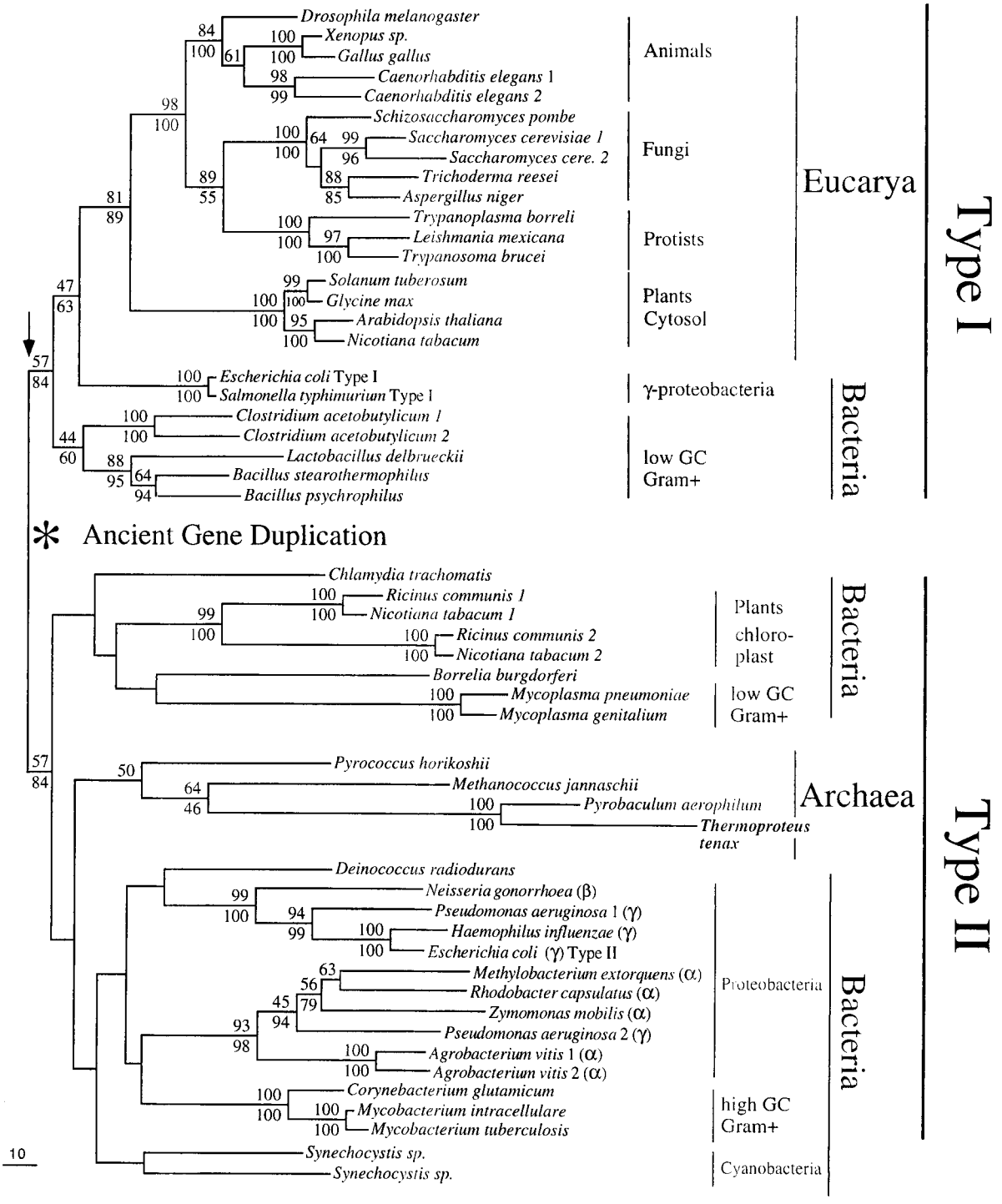

FIG. 6. Phylogenetic tree of PK. The tree was constructed by using the user-defined tree option of the MOLPHY package (1), based on the topology of the PAUP* Bootstrap Consensus tree (41). The numbers at certain nodes are bootstrap proportions; upper values correspond to the PAUP* Bootstrap analysis (500 replicates, four-times-random addition), and lower values correspond to the Kimura distance neighbor-joining analysis (1,000 replicates). Only values of >40% are shown in the figure. The sequence of the *T. tenax* PK is shown in boldface. The accession numbers for all PK sequences used for the phylogenetic analysis that were found in GenBank, in addition to sequences that were identified by BLAST search and downloaded at the NCBI, were as follows: *Xenopus* sp. (U03878), *Gallus gallus* (J00903), *Caenorhabditis elegans* 1 (Z69385), *Caenorhabditis elegans* 2 (Z81068), *Drosophila melanogaster* (AF06247), *Saccharomyces cerevisiae* 1 (U12980), *Saccharomyces cerevisiae* 2 (Z75255), *Trichoderma reesei* (L07060), *Aspergillus niger* (S38698), *Schizosaccharomyces pombe* (Z69380.1), *Trypanoplasma borrelii* (X77255), *Leishmania mexicana* (X74944), *Trypanosoma brucei* (X57951), *Solanum tuberosum* (cytosol, JC1481), *Glycine max* (cytosol, L08632), *Arabidopsis thaliana* (cytosol, AL022223), *Nicotiana tabacum* (cytosol, Z29492), *Escherichia coli* type I (AE000262), *Salmonella typhimurium* (X99945), *Bacillus stearothermophilus* (D13095), *Bacillus psychrophilus* (D31954), *Lactobacillus delbrueckii* (X71403), *Ricinus communis* 1 (chloroplast, M64737), *Nicotiana tabacum* 1 (chloroplast, Z28374), *Ricinus communis* 2 (chloroplast, M64736), *Nicotiana tabacum* 2 (chloroplast, Z28373), *Borrelia burgdorferi* (AE001141), *Mycoplasma pneumoniae* (AE000052), *Mycoplasma genitalium* (U39698), *Chlamydia trachomatis* (AE001306), *Methanococcus jannaschii* (U67468), *Pyrococcus horikoshii* (AP000002), *Haemophilus influenzae* (U32831), *Escherichia coli* type II (AE000279), *Agrobacterium vitis* 1 (U32375), *Agrobacterium vitis* 2 (U25634), *Methylobacterium extorquens* (U87316), *Zymomonas mobilis* (AF079586), *Mycobacterium intracellulare* (U65430), *Mycobacterium tuberculosis* (Z95554), *Corynebacterium glutamicum* (L27126), *Synechocystis* sp. strain 1 (D90907), and *Synechocystis* sp. strain 2 (D64004).

amino acid sequence FTKIV, which could be unequivocally assigned to the highly conserved first β-strand of the α/β_8-barrel of the catalytic PK domain A (bacterial consensus, TKI/LV/I), characterizing this region as an integral part of the coding gene. The close proximity of translation and transcription start of the *pyk* gene corresponds with the observation that especially some *Archaea* contain a high portion of mRNAs lacking Shine-Dalgarno sequences in front of the coding genes. The mechanism, however, allowing translation initiation independent of Shine-Dalgarno motifs is still unknown (7).

Northern blot analyses and primer extension studies suggest that the *pyk* gene of *T. tenax* is preferably transcribed under heterotrophic growth conditions supporting the catabolic function of the enzyme. Determination of the transcription start point, together with the length of the predominant transcript observed in Northern blot studies, suggest that the *pyk* transcript is monocistronic.

Phylogeny. One of the most striking features of the phylogenetic tree based on PK sequences is its dichotomic topology. Interestingly, this topology coincides with the differentiation of PK enzymes into two basic phenotypes. Thus, as known so far, all PK cluster I enzymes are active only in the presence of fructose-1,6-bisphosphate and/or other sugar phosphates, whereas the PK cluster II enzymes possess basal activity also without effectors but are mostly regulated by AMP and ATP, i.e., by the energy charge of the cell. The PK of *T. tenax* fits very well into this framework: like other PK II enzymes, the enzyme does not need heterotropic effectors for activity.

The dichotomic structure of the phylogenetic PK tree does not coincide with any of the four possible rooted universal tree topologies (9). The presence of PK enzymes from related bacteria (e.g., gamma proteobacteria or gram-positive bacteria) and even from the same organism (*E. coli*) in both clusters instead suggests that the dichotomic tree topology is caused by an early gene duplication event probably prior to the diversification of *Bacteria*. Since, however, in each cluster members of only two domains are present, we cannot definitely decide whether the two lineages trace back to the common ancestor or whether the duplication occurred after the domains had been segregated and the observed relationship is the result of lateral gene transfer events between domains. Examples of more recent gene duplication events are found in the lineages leading to *Caenorhabditis elegans*, *Saccharomyces cerevisiae*, *Clostridium acetobutylicum*, *Agrobacterium vitis*, and *Synechocystis* spp. *Pseudomonas aeruginosa* PK cluster II, which clusters with the alpha proteobacterial group, could serve as an example for a more recent lateral gene transfer.

For both eucaryal cytoplasmic PKs and archaeal enzymes, in contrast to *Bacteria*, only one PK isoform could be found: PK cluster I enzymes in *Eucarya* versus PK cluster II enzymes in *Archaea*. Because of the rather limited number of known PK sequences and completed genome projects in *Archaea*, we cannot clearly decide whether the second type is generally missing in that domain caused by an early loss or if it is just not yet detected due to the rather limited sequence information. The quite extensive data set for eucaryal PK seems to exclude the latter explanation for the exclusive occurrence of PK cluster I enzymes in the eucaryal cytoplasm, suggesting rather that *Eucarya* are, a priori, equipped only with one PK type, PK cluster I, probably inherited from an ancestral alpha proteobacterium via endosymbiosis. This assumption may explain the close affinity of the eucaryal and proteobacterial PKs documented in PK cluster I. Presumably, the PK cluster I encoding gene—like other genes coding for metabolic enzymes such as triosephosphate isomerase (20), GAPDH (16), and 3-PGK (3)—also represents a constituent of the bacterial inheritance of the eucaryal genome.

The rather poor resolution of the deeper rooting branches in PK cluster II leading to artificial associations may be, at least partially, caused by considerable differences in evolutionary rates of the PK sequences. Thus, unexpectedly, according to both parsimony and distance matrix analyses, the plastid PKs do not cluster together with the enzymes from cyanobacteria, whereas the monophyly of *Archaea* could not be confirmed by distance matrix and ML analyses. Possibly, the high evolutionary rates of the enzymes from plastids and the pathogenic strains of *Borrelia*, *Chlamydia*, and *Mycoplasma* (due to adaptation to specific cellular environments) lead to long-branch attraction covering their true phylogenetic relationships and resulting in the observed association of both enzyme groups. On the other hand, the slower evolutionary rates of the *Pyrococcus* enzyme compared to those of *Methanococcus* and both crenarchaeotal species may be the cause for its separation from the archaeal cluster in distance matrix and ML analyses.

Physiological role. The PKs of *Bacteria* and *Eucarya* represent the second control point of the catabolic EMP pathway adjusting the level of glycolytic intermediates for degradation or biosynthetic purposes and, by controlling the flux through the pathway, also regulating the level of ATP and GTP in the cell. To adapt immediately to changing intracellular and extracellular conditions, the PK activity is, like the ATP-dependent PFK, controlled at the protein level, mainly by allosteric mechanisms, whereas long-term adaptation is achieved on the gene level. As a typical catabolic enzyme, the expression of its coding gene is significantly reduced under anabolic conditions to avoid futile cycling of PEP (8).

As found for bacterial and eucaryal systems, the PK activity in *T. tenax* is strongly regulated at the transcript level: in heterotrophically grown cells both *pyk*-specific mRNA and the specific enzyme activity are four times higher than in autotrophically grown cells, clearly underlining the catabolic role of the enzyme. In contrast, the *T. tenax* enzyme differs from most bacterial and eucaryal enzymes by its reduced allosteric regulation, which seems to be restricted to positive binding cooperativity for PEP and divalent metal cations. At least the cooperative binding of PEP could possess some physiological relevance by enabling the enzyme to switch on its activity only at a PEP concentration exceeding a certain threshold. Thus, from the kinetic properties of the enzyme, one could expect an accumulation of PEP and preceding intermediates only up to ~1 mM. Higher concentrations would activate the enzyme, leading to a concomitant decrease of the intermediate pools. Obviously, the limited regulation capacity of the *T. tenax* PK should only ascertain a minor accumulation of intermediates for biosynthetic purposes, but it does not allow a stronger dam of intermediates, which could drive the carbon flux into anabolic direction as assumed for the bacterial and eucaryal systems (24).

The absence of a stringent throttle valve as a regulatory unit at the last step of the pathway in *T. tenax*, which does not allow a considerable accumulation of intermediates, seems to be favorable under thermoadaptive aspects. Considering the heat instability of several glycolytic intermediates (PEP, 1,3-bisphosphoglycerate, glyceraldehyde-3-phosphate, and dihydroxyacetone phosphate), the accumulation of free intermediates at high temperatures would result in an accelerated loss of these compounds and must therefore be avoided. The integration of nonphosphorylating GAPDH (GAPN) in the catabolic route of glycolysis is an important feature of metabolic thermoadaptation. This enzyme seems to serve thermoadaptive purposes in a two-fold manner: (i) by its allosteric properties

(4) compensating not only the missing allosteric potential of the reversible PP_i-PFK but also the reduced regulatory potential of PK and thus allowing the catabolism to take place without a bottleneck at the last step and (ii) by avoiding the formation of the highly labile intermediate 1,3-bisphosphoglycerate. As outlined above, the direct oxidation of glyceraldehyde-3-phosphate to 3-phosphoglycerate by GAPN is paid for with the loss of 2 mol of ATP/mol of glucose, which could be gained by using the phosphorylating GAPDH. Possibly, the reduced energy yield of the catabolic EMP pathway in *T. tenax* is compensated for by using PP_i instead of ATP as phosphoryl donor for the PFK reaction. Thus, all three striking features, by which the catabolic EMP variant of *T. tenax* differs from the classic glycolytic pathway (PP_i-dependent PFK, nonphosphorylating GAPN, and weakly regulated PK), could be related to thermoadaptation. Pool determinations of the various intermediates, as well as kinetic and regulatory investigations with other EMP enzymes, will show whether the presumed thermoadaptive background of the EMP variant in *T. tenax* can be confirmed.

ACKNOWLEDGMENTS

We are indebted to Roland Schmid (Universität Osnabrück, Osnabrück, Germany) for protein sequencing.

The work was supported by grants of the Deutsche Forschungsgemeinschaft and the Fonds der Chemischen Industrie.

REFERENCES

1. **Adachi, J., and M. Hasegawa.** 1996. MOLPHY version 2.3: programs for molecular phylogenetics based on maximum likelihood. Computer Science Monographs no. 28. Institute of Statistical Mathematics, Tokyo, Japan.
2. **Branny, P., F. de la Torre, and J.-F. Garel.** 1996. The genes for phosphofructokinase and pyruvate kinase of *Lactobacillus delbrueckii* subsp. *bulgaricus* constitute an operon. J. Bacteriol. **178:**4727–4730.
3. **Brinkmann, H., and W. Martin.** 1996. Higher-plant chloroplast and cytosolic 3-phosphoglycerate kinases: a case of endosymbiotic gene replacement. Plant Mol. Biol. **30:**65–75.
4. **Brunner, N. A., H. Brinkmann, B. Siebers, and R. Hensel.** 1998. NAD^+-dependent glyceraldehyde-3-phosphate dehydrogenase from *Thermoproteus tenax*: the first identified member of the aldehyde dehydrogenase superfamily is a glycolytic enzyme with unusual regulatory properties. J. Biol. Chem. **273:**6149–6156.
5. **Bult, C. J., O. White, G. J. Olsen, L. Zhou, R. D. Fleischmann, G. G. Sutton, J. A. Blake, L. M. Fitzgerald, R. A. Clayton, J. D. Gocayne, A. R. Kervelage, B. A. Dougherty, J.-F. Tomb, M. D. Adams, C. I. Reich, R. Overbeek, E. F. Kirkness, K. G. Weinstock, J. M. Merrick, A. Glodek, J. L. Scott, N. S. M. Geoghagen, J. F. Weidman, J. L. Fuhrmann, D. Nguyen, T. R. Utterback, J. M. Kelley, J. D. Peterson, P. W. Sadow, M. C. Hanna, M. D. Cotton, K. M. Roberts, M. A. Hurst, B. P. Kaine, M. Borodovsky, H.-P. Klenk, C. M. Fraser, H. O. Smith, C. R. Woese, and J. C. Venter.** 1996. Complete genome sequence of the methanogenic archaeon, *Methanococcus jannaschii*. Science **273:**1058–1073.
6. **Chomczynski, P.** 1992. One-hour downward alkaline capillary transfer for blotting of DNA and RNA. Anal. Biochem. **14:**134–139.
7. **Condo, I., A. Ciammaruconi, D. Benelli, D. Ruggero, and P. Londei.** 1999. *cis*-acting signals controlling translational initiation in the thermophilic archaeon *Sulfolobus solfataricus*. Mol. Microbiol. **34:**377–384.
8. **DeRisi, J. L., V. R. Iyer, and P. O. Brown.** 1997. Exploring the metabolic and genetic control of gene expression on a genomic scale. Science **278:**680–686.
9. **Doolittle, W. F., and J. R. Brown.** 1994. Tempo, mode, the progenote, and the universal root. Proc. Natl. Acad. Sci. USA **91:**6721–6728.
10. **Eckerskorn, C., W. Mewes, H. Goretzki, and F. Lottspeich.** 1988. A new siliconized glass fiber as support for chemical analysis of electroblotted proteins. Eur. J. Biochem. **176:**509–519.
11. **Fitz-Gibbon, S., A. J. Choi, J. H. Miller, K. O. Stetter, M. I. Simon, R. Swanson, and U. J. Kim.** 1997. A fosmid-based genomic map and identification of 474 genes of the hyperthermophilic archaeon *Pyrobaculum aerophilum*. Extremophiles **1:**36–51.
12. **Fothergill-Gilmore, L. A., and P. A. M. Michels.** 1993. Evolution of glycolysis. Prog. Biophys. Mol. Biol. **59:**105–235.
13. **Fürste, J. P., W. Pansegrau, R. Frank, H. Blöcker, P. Scholz, M. Bagdasarian, and E. Lanka.** 1986. Molecular cloning of the plasmid RP4 primase region in a multi-host-range *tacP* expression vector. Gene **48:**119–131.
14. **Görg, A., W. Postel, and S. Günther.** 1988. Two-dimensional electrophoresis. The current state of two-dimensional electrophoresis with immobilized pH gradients. Electrophoresis **9:**531–546.
15. **Hensel, R., S. Laumann, J. Lang, H. Heumann, and F. Lottspeich.** 1987. Characterization of two D-glyceraldehyde-3-phosphate dehydrogenases from the extremely thermophilic archaebacterium *Thermoproteus tenax*. Eur. J. Biochem. **170:**325–333.
16. **Hensel, R., P. Zwickl, S. Fabry, J. Lang, P. Palm.** 1989. Sequence comparison of glyceraldehyde-3-phosphate dehydrogenases from the three urkingdoms: evolutionary implication. Can. J. Microbiol. **35:**81–85.
17. **Jetten, M. S., M. E. Gubler, S. H. Lee, and A. J. Sinskey.** 1994. Structural and functional analysis of pyruvate kinase from *Corynebacterium glutamicum*. Appl. Environ. Microbiol. **60:**2501–2507.
18. **Jurica, M. S., A. Mesecar, P. J. Heath, W. Shi, N. Nowak, and B. L. Stoddard.** 1998. The allosteric regulation of pyruvate kinase by FBP. Structure **6:**195–210.
19. **Kawarabayasi, Y., M. Sawada, H. Horikawa, Y. Haikawa, Y. Hino, S. Yamamoto, M. Sekine, S. Baba, H. Kosugi, A. Hosoyama, Y. Nagai, M. Sakai, K. Ogura, R. Otuka, H. Nakazawa, M. Takamiya, Y. Ohfuku, T. Funahashi, T. Tanaka, Y. Kudoh, J. Yamazaki, N. Kushida, A. Oguchi, K. Aoki, Y. Nakamura, T. F. Robb, K. Horikoshi, Y. Masuchi, H. Shizuya, and H. Kikuchi.** 1998. Complete sequence and gene organization of the genome of a hyperthermophilic archaebacterium, *Pyrococcus horikoshii* OT3. DNA Res. **5:**55–76.
20. **Keeling, P. J., and W. F. Doolittle.** 1997. Evidence that eukaryotic triosephosphate isomerase is of alpha-proteobacterial origin. Proc. Natl. Acad. Sci. USA **94:**1270–1275.
21. **Kuo, Y. P., D. K. Thompson, A. St. Jean, R. L. Charlebois, and C. J. Daniels.** 1997. Characterization of two heat shock genes from *Haloferax volcanii*: a model system for transcription regulation in the *Archaea*. J. Bacteriol. **179:**6318–6324.
22. **Laemmli, U. K.** 1970. Cleavage of structural proteins during the assembly of the head of bacteriophage T4. Nature **277:**680–685.
23. **Larsen, T. M., M. M. Benning, I. Rayment, and G. H. Reed.** 1998. Structure of the bis(Mg^{2+})-ATP-oxalate complex of the rabbit muscle pyruvate kinase at 2.1 Å resolution: ATP binding over a barrel. Biochemistry **37:**6247–6255.
24. **Larsen, T. M., L. T. Laughlin, H. M. Holden, I. Rayment, and G. H. Reed.** 1994. Structure of rabbit muscle pyruvate kinase complexed with Mn^{2+}, K^+, and pyruvate. Biochemistry **33:**6301–6309.
25. **Leinfelder, W., M. Jarsch, and A. Böck.** 1985. The phylogenetic position of the sulfur-dependent archaebacterium *Thermoproteus tenax*: sequence of its 16S rRNA gene. System. Appl. Microbiol. **6:**164–170.
26. **Mattevi, A., G. Valentini, M. Rizzi, M. L. Speranza, M. Bolognesi, and A. Coda.** 1995. Crystal structure of *Escherichia coli* pyruvate kinase type I: molecular basis of the allosteric transition. Structure **3:**729–41.
27. **Matsudaira, P.** 1990. Limited N-terminal sequence analysis. Methods Enzymol. **182:**602–613.
28. **Meakin, S. A., J. Nash, W. D. Murray, K. J. Kennedy, and G. D. Sprott.** 1991. A generally applicable technique for the extraction of restrictable DNA from methanogenic bacteria. J. Microbiol. Methods **14:**119–126.
29. **Muirhead, H., D. A. Clayden, D. Barford, C. G. Lorimer, L. A. Fothergill-Gilmore, E. Schiltz, and W. Schmitt.** 1986. The structure of cat muscle pyruvate kinase. EMBO J. **5:**475–481.
30. **Nairn, J., D. Duncan, L. M. Gray, G. Urquhart, M. Binnie, O. Byron, L. A. Fothergill-Gilmore, and N. C. Price.** 1998. Purification and characterization of pyruvate kinase from *Schizosaccharomyces pombe*: evidence for an unusual quaternary structure. Protein Exp. Purif. **14:**247–253.
31. **Nairn, J., S. Smith, P. J. Allison, D. Rigden, L. A. Fothergill-Gilmore, and N. C. Price.** 1995. Cloning and sequencing of a gene encoding pyruvate kinase from *Schizosaccharomyces pombe*: implications for quaternary structure and regulation of the enzyme. FEMS Microbiol. Lett. **134:**221–226.
32. **Pawluk, A., R. K. Scopes, and K. Griffiths-Smith.** 1986. Isolation and properties of the glycolytic enzymes from *Zymomonas mobilis*. The five enzymes from glyceraldehyde-3-phosphate dehydrogenase through to pyruvate kinase. Biochem. J. **238:**275–281.
33. **Philippe, H.** 1993. MUST, a computer package of management utilities for sequences and trees. Nucleic Acids Res. **21:**5264–5272.
34. **Potter, S., and L. A. Fothergill-Gilmore.** 1992. Purification and properties of pyruvate kinase from *Thermoplasma acidophilum*. FEMS Microbiol. Lett. **94:**235–240.
35. **Saitou, N., and M. Nei.** 1987. The neighbor-joining method: a new method for reconstructing phylogenetic trees. Mol. Biol. Evol. **4:**406–425.
36. **Sambrook, J., E. F. Fritsch, and T. Maniatis.** 1989. Molecular cloning: a laboratory manual, 2nd ed. Cold Spring Harbor Laboratory Press, Cold Spring Harbor, N.Y.
37. **Selig, M., K. B. Xavier, H. Santos, and P. Schönheit.** 1997. Comparative analysis of Embden-Meyerhof and Entner-Doudoroff glycolytic pathways in hyperthermophilic archaea and the bacterium *Thermotoga*. Arch. Microbiol. **167:**217–232.
38. **Siebers, B., and R. Hensel.** 1993. Glucose catabolism of the hyperthermophilic archaeum *Thermoproteus tenax*. FEMS Microbiol. Lett. **111:**1–8.
39. **Siebers, B., H.-P. Klenk, and R. Hensel.** 1998. PPi-dependent phosphofructokinase from *Thermoproteus tenax*, an archaeal descendant of an ancient line in phosphofructokinase evolution. J. Bacteriol. **180:**2137–2143.
40. **Siebers, B., V. F. Wendisch, and R. Hensel.** 1997. Carbohydrate metabolism

in *Thermoproteus tenax: in vivo* utilization of the non-phosphorylative Entner-Doudoroff pathway and characterization of its first enzyme, glucose dehydrogenase. Arch. Microbiol. **168:**120–127.
41. **Swofford, D. L.** 1999. PAUP*: phylogenetic analysis using parsimony (and other methods), version 4.0. Sinauer Associates, Sunderland, Mass.
42. **Thompson, J. D., D. G. Higgins, and T. J. Gibson.** 1994. CLUSTAL W: improving the sensitivity of progressive multiple sequence alignment through sequence weighting, position-specific gap penalties and weight matrix choice. Nucleic Acids Res. **22:**4673–4680.
43. **van der Oost, J., G. Schut, S. W. Kengen, W. R. Hagen, M. Thomm, and W. M. de Vos.** 1998. The ferredoxin-dependent conversion of glyceraldehyde-3-phosphate in the hyperthermophilic archaeon *Pyrococcus furiosus* represents a novel site of glycolytic regulation. J. Biol. Chem. **273:**28149–28154.
44. **Weil, C. F., D. S. Cram, B. A. Sherf, and J. N. Reeve.** 1988. Structure and comparative analysis of the genes encoding components C of methyl coenzyme M reductase in the extremely thermophilic archaebacterium *Methanothermus fervidus*. J. Bacteriol. **70:**4718–4726.
45. **Zillig, W., K. O. Stetter, W. Schäfer, D. Janekovic, S. Wunderl, I. Holz, and P. Palm.** 1981. Thermoproteales: a novel type of extremely thermophilic anaerobic archaebacteria isolated from Icelandic solfatares. Zentbl. Bakteriol. Hyg. I Abt. Orig. C **2:**205–227.